0026-895X/08/7406-1687–1695$20.00
MOLECULAR PHARMACOLOGY
Copyright © 2008 The American Society for Pharmacology and Experimental Therapeutics
Mol Pharmacol 74:1687–1695, 2008

Vol. 74, No. 6
50500/3411024
Printed in U.S.A.

Tryptophan Mutations at Azi-Etomidate Photo-Incorporation Sites on α_1 or β_2 Subunits Enhance $GABA_A$ Receptor Gating and Reduce Etomidate Modulation

Deirdre Stewart, Rooma Desai, Qi Cheng,[1] Aiping Liu, and Stuart A. Forman

Beecher-Mallincrodt Laboratories, Department of Anesthesia & Critical Care, Massachusetts General Hospital, Boston, Massachusetts

Received July 14, 2008; accepted September 18, 2008

ABSTRACT

The potent general anesthetic etomidate produces its effects by enhancing $GABA_A$ receptor activation. Its photolabel analog [^{3}H]azi-etomidate labels residues within transmembrane domains on α and β subunits: αMet236 and βMet286. We hypothesized that these methionines contribute to etomidate sites formed at α-β subunit interfaces and that increasing side-chain bulk and hydrophobicity at either locus would mimic etomidate binding and block etomidate effects. Channel activity was electrophysiologically quantified in $\alpha_1\beta_2\gamma_{2L}$ receptors with α_1M236W or β_2M286W mutations, in both the absence and the presence of etomidate. Measurements included spontaneous activation, GABA EC_{50}, etomidate agonist potentiation, etomidate direct activation, and rapid macrocurrent kinetics. Both α_1M236W and β_2M286W mutations induced spontaneous channel opening, lowered GABA EC_{50}, increased maximal GABA efficacy, and slowed current deactivation, mimicking effects of etomidate on $\alpha_1\beta_2\gamma_{2L}$ channels. These changes were larger with α_1M236W than with β_2M286W. Etomidate (3.2 μM) reduced GABA EC_{50} much less in α_1M236W$\beta_2\gamma_{2L}$ receptors (2-fold) than in wild type (23-fold). However, etomidate was more potent and efficacious in directly activating α_1M236W$\beta_2\gamma_{2L}$ compared with wild type. In $\alpha_1\beta_2$M286Wγ_{2L} receptors, etomidate induced neither agonist-potentiation nor direct channel activation. These results support the hypothesis that α_1Met236 and β_2Met286 are within etomidate sites that allosterically link to channel gating. Although α_1M236W produced the larger impact on channel gating, β_2M286W produced more profound changes in etomidate sensitivity, suggesting a dominant role in drug binding. Furthermore, quantitative mechanistic analysis demonstrated that wild-type and mutant results are consistent with the presence of only one class of etomidate sites mediating both agonist potentiation and direct activation.

Etomidate is a potent intravenous general anesthetic that produces its behavioral effects via ionotropic GABA type A ($GABA_A$) receptors, the major inhibitory postsynaptic ion channels in mammalian brain (Jurd et al., 2003; Reynolds et al., 2003). $GABA_A$ receptors contain a central chloride ion channel surrounded by five homologous subunits, each with a large amino-terminal extracellular domain, four transmembrane domains (M1–M4), and a large intracellular domain between M3 and M4 (Sieghart, 2006). Eighteen mammalian $GABA_A$ receptor subunits have been identified, but only a few combinations are widely expressed in neurons. Etomidate acts selectively on $GABA_A$ receptors containing β_2 and β_3 subunits (Hill-Venning et al., 1997), including $\alpha_1\beta_2\gamma_{2L}$, the most abundant receptor subtype.

A photoactivatable etomidate analog, [^{3}H]azi-etomidate (Husain et al., 2003; Liao et al., 2005), labels affinity-purified bovine $GABA_A$ receptors both at βMet286 in M3 and at αMet236 in M1 (Li et al., 2006), suggesting that etomidate sites are formed within transmembrane α-β interfacial pockets. The subunit stoichiometry of 2α:2β:1γ (Chang et al., 1996) together with the arrangement of $GABA_A$ receptor subunits (Baumann et al., 2002) predict two interfacial etomidate sites per channel.

From an electrophysiological perspective, etomidate and azi-etomidate slow decay of neuronal IPSCs and similarly slow deactivation of $GABA_A$ receptor-mediated macrocurrents elicited with brief agonist pulses (Yang and Uchida, 1996; Zhong et al., 2008). Etomidate potentiates currents elicited by submaximal GABA, shifting GABA EC_{50} to lower concentrations. High concentrations of etomidate or azi-etomidate also directly activate $GABA_A$ receptors. Similar ac-

This research was supported by grants from the National Institutes of General Medical Sciences (R01-GM66724 and P01-GM58448).

These results were presented in part and in preliminary form at the American Society of Anesthesiologists Annual Meeting (October 2007, San Francisco, CA) and at the Society for Neuroscience Annual Meeting (November 2007, San Diego, CA).

[1] Current affiliation: Nathan Kline Institute, Orangeburg, New York.

Article, publication date, and citation information can be found at http://molpharm.aspetjournals.org.
doi:10.1124/mol.108.050500.

ABBREVIATIONS: $GABA_A$, GABA type A; PTX, picrotoxin; ETO, etomidate; HEK, human embryonic kidney; P_o, open probability.

tions on $GABA_A$ receptors are produced by barbiturates (Serafini et al., 2000), propofol and its analogs (Krasowski et al., 2002), and neuroactive steroid anesthetics (Majewska et al., 1986; Hosie et al., 2006). In $\alpha_1\beta_2\gamma_{2L}$ $GABA_A$ receptors, both direct activation and agonist potentiation by etomidate are quantitatively accounted for by an allosteric model with two equivalent sites linked to channel gating (Rusch et al., 2004). Alternatively, two distinct types of sites may exist for etomidate and/or other potent anesthetics: high-affinity agonist potentiation sites and low-affinity direct activation sites. Indeed, Hosie et al. (2006) reported that mutations in the α-β transmembrane interface (near the azi-etomidate photolabeled residues) selectively alter direct neuroactive steroid activation of $GABA_A$ receptors, whereas other sites affect potentiation.

Mutations at βMet286 have been studied previously, focusing on altered sensitivity to the GABA-potentiating effects of anesthetics and neuroactive steroids (Krasowski et al., 1998; Krasowski et al., 2001; Siegwart et al., 2002). However, the impact of mutations at α_1Met236 has not previously been reported.

Here, we report studies of the role of αMet236 and βMet286 in both gating and etomidate sensitivity in $\alpha_1\beta_2\gamma_{2L}$ $GABA_A$ receptors. We compared in detail the functional impact of α_1M236W and β_2M286W mutations, postulating that a large hydrophobic side-chain would mimic the presence of etomidate within the α-β interface. Mutant and wild-type receptors were expressed in HEK293 cells and *Xenopus laevis* oocytes. $GABA_A$ receptor-mediated currents in oocytes were quantified to determine GABA concentration responses in the absence and presence of etomidate, direct activation of channels by etomidate, spontaneous channel activity, and the maximum efficacy of GABA gating. Receptors in HEK293 membrane patches were activated using ultra-fast GABA concentration jumps to measure macrocurrent activation, desensitization, and deactivation rates.

Both α_1M236W and β_2M286W mutations produced qualitatively similar but quantitatively different changes in $GABA_A$ receptor gating in the absence of etomidate. Etomidate modulation of GABA responses was also reduced by both mutations, but each mutation had distinct effects on direct receptor activation: α_1M236W enhanced etomidate agonism, whereas β_2M286W eliminated this action. Nonetheless, quantitative mechanistic analysis of both mutant data sets remains consistent with an allosteric coagonist model in which all etomidate effects are mediated by one class of sites.

Materials and Methods

Animal Use. Female *X. laevis* were housed in a veterinary-supervised environment in accordance with local and federal guidelines. Frogs were anesthetized by immersion in ice-cold 0.2% tricaine (Sigma-Aldrich, St. Louis, MO) before mini-laparotomy to harvest oocytes.

Chemicals. *R*(+)-Etomidate was obtained from Bedford Laboratories (Bedford, OH). The clinical preparation in 35% propylene glycol was diluted directly into buffer. Previous studies have shown that propylene glycol at the dilutions used for these studies has no effect on $GABA_A$ receptor function (Rusch et al., 2004). Picrotoxin (PTX) was purchased from Sigma-Aldrich (St. Louis, MO) and dissolved in electrophysiology buffer (2 mM) by prolonged gentle shaking. Alphaxalone was purchased from MP Biomedicals (Solon, OH) and prepared as a stock solution in dimethyl sulfoxide. Salts and buffers were purchased from Sigma-Aldrich.

Molecular Biology. cDNAs for human $GABA_A$ receptor α_1, β_2, and γ_{2L} subunits were cloned into pCDNA3.1 vectors (Invitrogen, Carlsbad, CA). To create α_1M236W and β_2M286W mutations in cDNA, oligonucleotide-directed mutagenesis was performed using QuikChange kits (Stratagene, La Jolla, CA). Clones from each mutagenesis reaction were subjected to DNA sequencing through the entire cDNA region to confirm the presence of the mutation and absence of stray mutations.

Expression of $GABA_A$ Receptors. Messenger RNA was synthesized in vitro from linearized cDNA templates and purified using commercial kits (Ambion Inc., Austin, TX). Subunit mRNAs were mixed at 1α:1β and at least 2-fold excess γ to promote homogeneous receptor expression (Boileau et al., 2002, 2003). mRNA mixture [25 to 50 nl (15–25 ng)] was microinjected into *X. laevis* oocytes, and they were then incubated at 18°C in ND96 (96 mM NaCl, 2 mM KCl, 0.8 mM $MgCl_2$, 1.8 mM $CaCl_2$, and 5 mM HEPES, pH 7.5) supplemented with gentamicin (0.05 mg/ml) for 24 to 48 h before electrophysiology. HEK293 cells were cultured on glass coverslips, maintained as described previously (Scheller and Forman, 2002), and transfected with plasmids encoding $GABA_A$ receptor subunit mixtures (1α:1β:2γ) using Lipofectamine (Invitrogen, Carlsbad, CA). A eukaryotic green fluorescent protein expression plasmid, pmaxGFP (Amaxa, Gaithersburg, MD), was mixed with the $GABA_A$ receptor subunit plasmids to aid in identification of transfected cells. Transfected cells were maintained in culture medium for 24 to 48 h before electrophysiology experiments.

Oocyte Electrophysiology. $GABA_A$ receptor responses to GABA were assessed in *X. laevis* oocytes using two-microelectrode voltage-clamp electrophysiology, as described previously (Rusch and Forman, 2005). GABA pulses lasted from 5 to 20 s, depending on the concentration of GABA used and the time to steady-state peak current. Normalizing GABA responses, usually at maximal GABA (1–10 mM), were recorded every 2nd or 3rd sweep. Picrotoxin-sensitive leak currents were measured by superfusion with 2 mM PTX, followed by washout for at least 5 min before testing maximal GABA response. Alphaxalone (2 μM) was used as a gating enhancer in combination with 10 mM GABA, to provide estimates of GABA efficacy. Oocyte currents were low-pass-filtered at 1 kHz (model OC-725B; Warner Instruments, Hamden, CT) and digitized at 1 to 2 kHz using commercial digitizer hardware (Digidata 1200; Molecular Devices, Sunnyvale, CA) and software (pClamp 7; Molecular Devices).

Electrophysiology in HEK293 Cell Membrane Patches. Current recordings from excised outside-out membrane patches were performed at −50 mV and room temperature (21–23°C) as described previously (Scheller and Forman, 2002). Bath and superfusion solutions contained 145 mM NaCl, 5 mM KCl, 10 mM HEPES, 2 mM $CaCl_2$, and 1 mM $MgCl_2$ at pH 7.4 (pH adjusted with *N*-methyl glucosamine). The intracellular (pipette) fluid contained 140 mM KCl, 10 mM HEPES, 1 mM EGTA, and 2 mM $MgCl_2$ at pH 7.3 (pH adjusted with KOH). Currents were stimulated using brief (0.5–1.0 s) pulses of GABA delivered via a quad (2 × 2) superfusion pipette coupled to piezoelectric elements that switched superfusion solutions in under 1 ms. Currents were filtered at 5 kHz and digitized at 10 kHz for off-line analysis.

Data Analysis. Leak-correction and measurement of peak currents was performed off-line using Clampfit 8.0 software (Molecular Devices). Peak GABA- or etomidate-activated oocyte currents were normalized to maximal GABA-activated currents measured in the same cell (I_{max}^{GABA}). Concentration-response curves were assembled from pooled normalized data from multiple oocytes. Pooled data sets were fitted with logistic functions using nonlinear least-squares (Origin 6.1; OriginLab Corp., Northampton, MA):

$$\frac{I}{I_{max}^{GABA}} = A \times \frac{[\text{Agonist}]^{n_H}}{[\text{Agonist}]^{n_H} + EC_{50}^{n_H}} \quad (1)$$

where A is amplitude and n_H is Hill slope.

Etomidate potentiation of GABA responses was quantified as the ratio of the GABA EC_{50} values in the absence of drug to that in the presence of drug. GABA concentration-response curves shift leftward (i.e., to a lower GABA EC_{50}) in the presence of etomidate; thus, large EC_{50} ratios indicate strong modulation whereas a ratio of 1.0 or less indicates no positive modulation.

PTX-sensitive leak currents (I_{PTX}) were normalized to I_{max}^{GABA}, providing estimates of basal open probability (P_o). Maximal GABA efficacy was assessed by first activating oocyte-expressed channels with 10 mM GABA. After full current activation and initial desensitization, superfusate was switched to 10 mM GABA plus 2 μM alphaxalone, a potent and efficacious positive modulator of wild-type and the mutant receptors. Maximal GABA efficacy was calculated as the ratio of current immediately before the addition of alphaxalone (I_{max}^{GABA}) to the secondary current peak after the addition of alphaxalone ($I^{GABA+alphax}$).

Estimated P_o was calculated by explicitly adding spontaneous current and renormalizing to the full range of open probability, assuming that PTX-blocked leak represents no activation and maximal GABA plus alphaxalone activates all channels:

$$P_o^{est} = \frac{\frac{I}{I_{max}^{GABA}} + \frac{I_{PTX}}{I_{max}^{GABA}}}{\frac{I^{GABA+Alphax}}{I_{max}^{GABA}} + \frac{I_{PTX}}{I_{max}^{GABA}}} \quad (2)$$

Quantitative analysis based on Monod-Wyman-Changeux coagonism was performed as follows: Estimated P_o data from GABA concentration-responses (with and without etomidate) and etomidate direct activation data were pooled. With both [GABA] and [ETO] specified as independent variables, these data were globally fitted to eq. 3 using nonlinear least-squares:

$$P_o = \frac{1}{1 + L_0\left(\frac{1 + [GABA]/K_G}{1 + [GABA]/cK_G}\right)^2\left(\frac{1 + [ETO]/K_E}{1 + [ETO]/dK_E}\right)^2} \quad (3)$$

This equation describes an allosteric two-state equilibrium mechanism with two classes of agonist sites (one for GABA and one for etomidate), each with two equivalent sites. L_0 in eq. 3 is a dimensionless basal equilibrium gating variable, approximately P_o^{-1}. K_G and K_E are equilibrium dissociation constants for GABA and etomidate binding to inactive states, and c and d are dimensionless parameters representing the respective ratios of binding constants in active versus inactive states. The agonist efficacy of GABA and etomidate are inversely related to c and d, respectively,.

To analyze membrane patch macrocurrents for activation, desensitization, and deactivation kinetics, data windows were specified in each trace for different phases of the wave form. Activation windows were from 10% above the baseline trace to a point where desensitization had reduced the peak current by 3 to 5%. Desensitization windows were from the current peak to the end of GABA application. Deactivation windows were from the end of GABA application to the end of the sweep. Windowed data were fitted to multiple exponential functions using nonlinear least-squares:

$$I(t) = A_1 \times \exp(-t/\tau_1) + A_2 \times \exp(-t/\tau_2) + A_3 \times \exp(-t/\tau_3) + C \quad (4)$$

The number of components for each fit was determined by comparison of single-, double-, and triple-exponential fits, using an F statistic to choose the best exponential fit model with a confidence value of $P = 0.99$ (Clampfit 8.0). All activation traces were best fit with a single exponent, whereas desensitization was consistently fitted with two exponents. Wild-type and $\alpha_1\beta_2$M286W$\gamma 2_L$ deactivation were best fitted with two exponents, and α_1M236W$\beta_2\gamma_{2L}$ deactivation was best fit with a single exponent in all but one trace ($n = 8$).

Statistical Analysis. Results are reported as mean ± S.D. unless otherwise indicated. Group comparisons were performed using either a two-tailed Student's t test (with independent variances) or analysis of variance with Tukey's post hoc multiple comparisons test in MS Excel 2003 (Microsoft Corp., Redmond, WA) with an add-on statistical toolkit (StatistiXL, http://www.statistixl.com).

Results

GABA Concentration Responses in the Absence and Presence of Etomidate. Both tryptophan mutations, when expressed in the $\alpha_1\beta_2\gamma_{2L}$ background, formed functional GABA-activated ion channels in both *X. laevis* oocytes and HEK293 cells. The wild-type GABA EC_{50} from a logistic fit to pooled oocyte normalized peak current data was 43 μM (Fig. 1A, Table 1). Compared with wild-type $GABA_A$ receptors, both α_1M236W$\beta_2\gamma_{2L}$ and $\alpha_1\beta_2$M286Wγ_{2L} receptors displayed significantly increased sensitivity to GABA. GABA EC_{50} values were approximately 20-fold lower for α_1M236W$\beta_2\gamma_{2L}$ (2 μM) and 6-fold lower for $\alpha_1\beta_2$M286Wγ_{2L} (7 μM) (Fig. 1, B and C; Table 1). GABA EC_{50} for wild-type and α_1M236W$\beta_2\gamma_{2L}$ receptors were also measured in HEK293 membrane patches using rapid-superfusion and patch-clamp electrophysiology. In these experiments, wild-type GABA $EC_{50} = 44 \pm 8.5$ μM ($n = 4$) and α_1M236W$\beta_2\gamma_{2L}$ GABA $EC_{50} = 2.6 \pm 0.83$ μM ($n = 4$), values not significantly different from those from *X. laevis* oocyte experiments.

In oocytes expressing wild-type receptors, addition of 3.2 μM etomidate enhanced responses to low GABA, reducing GABA EC_{50} from 43 to 1.9 μM (23-fold). Etomidate also increased the maximal response to GABA (1–10 mM) by

TABLE 1

Wild-type and mutant channel gating characteristics

Results are derived from oocyte electrophysiology experiments. Maximal GABA efficacy was estimated using alphaxalone as a positive modulator, assuming that 100% activation occurred in the presence of 10 mM GABA + alphaxalone. Etomidate efficacy is normalized to maximal GABA. EC_{50} ratios are calculated as the GABA EC_{50} in the absence of etomidate divided by that in the presence of 3.2 μM etomidate, reported in the legend to Figure 1.

Receptor	GABA EC_{50}	Max. GABA Efficacy	ETO EC_{50} (μM)	ETO Efficacy	Spontaneous Activity	EC_{50} Ratio (Control/3.2 μM ETO)
	μM	%	μM	%	%	
$\alpha_1\beta_2\gamma_{2L}$	43 ± 1.7 ($n = 10$)	88 ± 3.0 ($n = 8$)	31 ± 12 ($n = 5$)	39 ± 6.2 ($n = 5$)	<0.1 ($n = 5$)	23 ± 1.7 ($n = 8$)
α_1M236W$\beta_2\gamma_{2L}$*	2.0 ± 0.10 ($n = 11$)	99 ± 1.2 ($n = 7$)	12 ± 2.7 ($n = 7$)	97 ± 7.2 ($n = 7$)	16 ± 2.9 ($n = 8$)	1.7 ± 0.26 ($n = 9$)
$\alpha_1\beta_2$M286Wγ_{2L}*	6.6 ± 1.3† ($n = 8$)	100 ± 0.3 ($n = 6$)			4.1 ± 0.81† ($n = 10$)	1.1 ± 0.31† ($n = 8$)

* All values for both mutants differ from wild-type at $P < 0.01$.
† Differs from α_1M236W$\beta_2\gamma_{2L}$ at $P < 0.01$.

approximately 20% (Fig. 1A). In α_1M236W$\beta_2\gamma_{2L}$ channels, etomidate enhanced GABA-activated currents much less than in wild-type. In the presence of 3.2 μM etomidate, the α_1M236W$\beta_2\gamma_{2L}$ GABA EC_{50} was 1.2 μM (Fig. 1B), only 1.7-fold lower than control (Table 1). No etomidate modulation of $\alpha_1\beta_2$M286Wγ_{2L} receptors was observed. GABA EC_{50} for $\alpha_1\beta_2$M286Wγ_{2L} receptors was not significantly reduced in the presence of 3.2 μM etomidate. Etomidate did not significantly increase maximal GABA responses in either mutant channel.

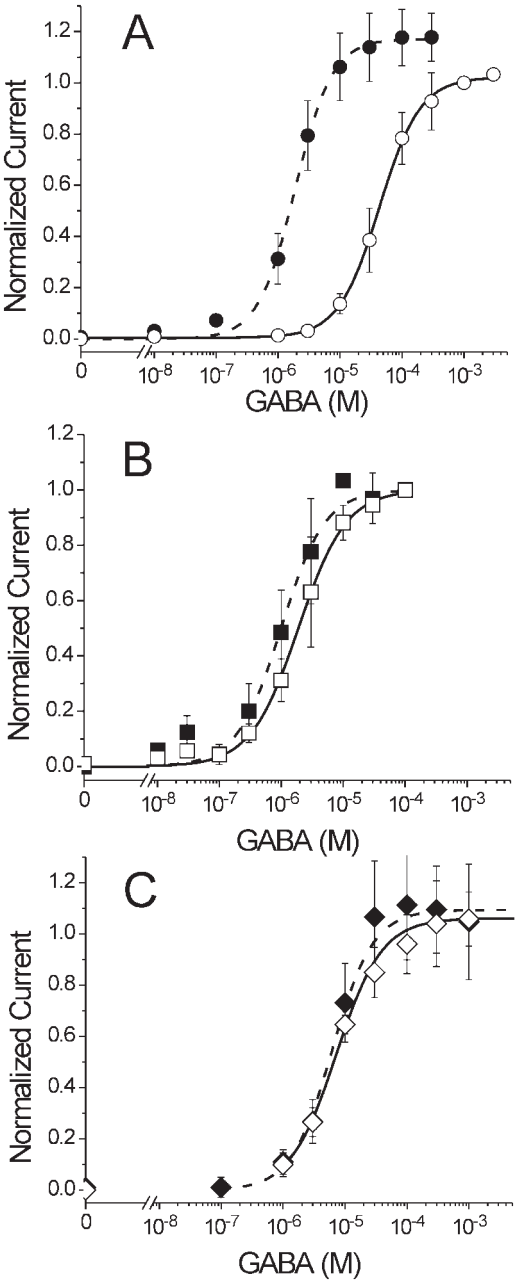

Fig. 1. GABA concentration-responses in the absence and presence of etomidate. Data points represent mean ± S.D. ($n \geq 8$) peak oocyte currents normalized to maximal GABA-elicited currents in the absence of etomidate. Open symbols represent control conditions and solid symbols represent experiments in the presence of 3.2 μM etomidate. Lines represent logistic (eq. 1) fits to data in the absence (solid) and presence (dashed) of etomidate. GABA EC_{50} ratios (control/3.2 μM ETO) are reported in Table 1. A, wild-type $\alpha_1\beta_2\gamma_{2L}$ receptors. Control (○), $A = 1.02 \pm 0.01$; $EC_{50} = 43 \pm 1.7$ μM; nH = 1.3 ± 0.12. 3.2 μM Eto (●), $A = 1.17 \pm 0.02$; $EC_{50} = 1.9 \pm 0.12$ μM; nH = 1.5 ± 0.13. B, α_1M236W$\beta_2\gamma_{2L}$ receptors. Control (□), $A = 1.00 \pm 0.013$; $EC_{50} = 2.0 \pm 0.10$ μM; $n_H = 1.2 \pm 0.11$. 3.2 μM Eto (■), $A = 0.98 \pm 0.023$; $EC_{50} = 1.2 \pm 0.18$ μM; $n_H = 1.4 \pm 0.25$. C, $\alpha_1\beta_2$M286Wγ_{2L} receptors. Control (◇), $A = 1.06 \pm 0.07$; $EC_{50} = 6.6 \pm 1.3$ μM; $n_H = 1.2 \pm 0.34$. 3.2 μM Eto (◆), $A = 1.09 \pm 0.11$; $EC_{50} = 6.2 \pm 2.1$ μM; $n_H = 1.3 \pm 0.36$.

Etomidate Direct Activation. Wild-type $\alpha_1\beta_2\gamma_{2L}$ $GABA_A$ receptors expressed in *X. laevis* oocytes were directly activated by etomidate at concentrations above 3 μM (Fig. 2). Maximal directly activated wild-type currents (at 100–320 μM etomidate) averaged around 40% of maximal GABA-activated currents. Logistic analysis of pooled oocyte peak currents elicited with etomidate gave a wild-type etomidate EC_{50} of 31 μM (Fig. 2; Table 1). The α_1M236W$\beta_2\gamma_{2L}$ receptors were also activated directly by etomidate. Maximal etomidate efficacy for α_1M236W$\beta_2\gamma_{2L}$ receptors was approximately the same as GABA (97%), and etomidate EC_{50} for this mutant was 12 μM (Fig. 2; Table 1), significantly lower than that for wild-type ($p < 0.01$). No etomidate-activated currents were observed in studies of $\alpha_1\beta_2$M286Wγ_{2L} receptors.

Spontaneous Receptor Activity. Wild-type $\alpha_1\beta_2\gamma_{2L}$ $GABA_A$ receptors have a very low P_o in the absence of agonist. P_o for these channels has been estimated at 1 to 5 × 10^{-5} (Chang and Weiss, 1999; Rusch et al., 2004; Rusch and Forman, 2005). Consistent with previous studies, we observed no picrotoxin-sensitive resting leak currents in oocytes expressing $\alpha_1\beta_2\gamma_{2L}$ receptors (Fig. 3, top; Table 1). However, mutations may induce spontaneous opening of $GABA_A$ receptor channels, and in these cases, P_o can be assessed using inhibitors such as picrotoxin (Chang and Weiss, 1999; Scheller and Forman, 2002). Oocytes expressing α_1M236W$\beta_2\gamma_{2L}$ receptors displayed large resting leak currents that were blocked by 2 mM PTX. The PTX-sensitive leak averaged 16% of maximal GABA-activated current (Fig. 3, top). Oocytes expressing $\alpha_1\beta_2$M286Wγ_{2L} receptors also displayed PTX-sensitive leak currents that were, on average, approximately 4% of maximal GABA-activated currents.

Estimation of Maximal GABA Efficacy. Etomidate increased $\alpha_1\beta_2\gamma_{2L}$ receptor currents elicited with maximal (3–10 mM) GABA by approximately 20% but was relatively

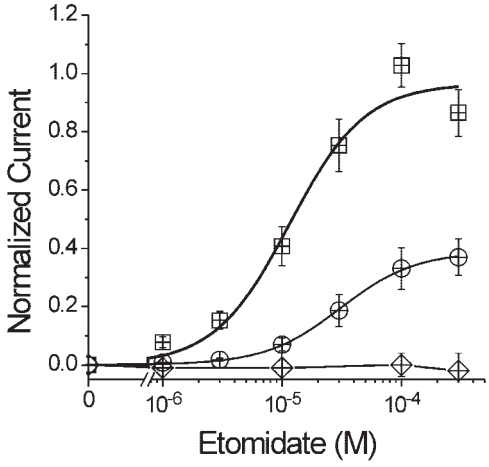

Fig. 2. Etomidate direct activation concentration-responses. Data points represent mean ± S.D. ($n > 5$) peak oocyte currents normalized to maximal GABA-elicited currents. Lines represent logistic (eq. 1) fits to data. Wild-type $\alpha_1\beta_2\gamma_{2L}$ receptors (○), $A = 0.39 \pm 0.062$; $EC_{50} = 31 \pm 12$ μM; $n_H = 1.3 \pm 0.23$. α_1M236W$\beta_2\gamma_{2L}$ receptors (□), $A = 0.97 \pm 0.072$; $EC_{50} = 12 \pm 2.7$ μM; $n_H = 1.5 \pm 0.21$. $\alpha_1\beta_2$M286Wγ_{2L} receptors (◇), no fit.

ineffective at enhancing even submaximal GABA-activated currents in mutant channels (Fig. 1). In contrast, the neuroactive steroid alphaxalone (2 μM) produced at least 2-fold enhancement of currents elicited with EC_{50} or lower GABA in oocytes expressing wild-type as well as mutant receptors (not shown). We therefore used alphaxalone to quantify maximal GABA efficacy for all three receptors using single-sweep multisolution experiments. After activation with 10 mM GABA, addition of 2 μM alphaxalone increased wild-type currents by the same amount observed using etomidate (i.e., 15 to 20%) (Fig. 3, bottom). Assuming that the alphaxalone-enhanced activation represents 100% open probability, we calculated average maximal efficacy of GABA in $\alpha_1\beta_2\gamma_{2L}$ receptors to be 88% (Table 1). For both α_1M236W$\beta_2\gamma_{2L}$ and $\alpha_1\beta_2$M286Wγ_{2L} receptors, alphaxalone minimally enhanced currents elicited with 10 mM GABA, suggesting that maximal GABA efficacy for these mutants is greater than 99% (Fig. 3, bottom; Table 1).

Macrocurrent Activation, Desensitization, and Deactivation Rates. Using a piezo-driven superfusion pipette capable of solution exchanges in approximately 0.2 ms, we elicited GABA-activated macrocurrents in voltage-clamped excised outside-out patches from HEK293 cells expressing $GABA_A$ receptors (Fig. 4). These currents were analyzed for activation, desensitization, and deactivation kinetics (Table 2). Wild-type $\alpha_1\beta_2\gamma_{2L}$ receptor currents displayed maximal activation rates averaging 2200 s^{-1}. Desensitization of wild-type receptor currents was biphasic, with 20% fast desensitization (τ_{fast} = 27 ms), and a dominant (80%) slow phase (τ_{slow} = 1100 ms). Deactivation of wild-type currents was biphasic, with τ_{fast} = 21 ms and τ_{slow} = 70 ms. Macrocurrents from both α_1M236W$\beta_2\gamma_{2L}$ and $\alpha_1\beta_2$M286Wγ_{2L} receptors displayed activation and desensitization rates that were similar to wild-type. In addition, currents from both mutant receptors displayed deactivation that was much slower than in wild-type currents. Macrocurrents recorded from patches expressing α_1M236W$\beta_2\gamma_{2L}$ were characterized by a single slow deactivation time constant, τ = 410 ms. Currents from patches expressing $\alpha_1\beta_2$M286Wγ_{2L} receptors deactivated biphasically: approximately 30% with a τ_{fast} = 96 ms and 70% with τ_{slow} = 430 ms.

Discussion

Tryptophan mutation at either azi-etomidate photoincorporation site (α_1Met236 or β_2Met286) produces changes in $GABA_A$ receptor gating that mimic the reversible actions of etomidate in wild-type $\alpha_1\beta_2\gamma_{2L}$ receptors. Both mutant channels display GABA EC_{50} values significantly lower than wild-type, increased maximal GABA efficacy, and spontaneous activity in the absence of orthosteric agonists. Spontaneous activation associated with a β_1M286W mutation was previously reported (Findlay et al., 2001), although this is the first report of spontaneous activity resulting from an α-M1 domain mutation. Macrocurrent kinetics in both mutant channels is characterized by normal activation and desensitization but much slower deactivation than wild type. The equilibrium and kinetic gating changes caused by α_1M236W and β_2M286W are identical to those observed in $\alpha_1\beta_2\gamma_{2L}$ $GABA_A$ receptors in the presence of etomidate or after photomodification with azi-etomidate (Zhong et al., 2008) and are probably due to stabilization of open channel states in both the absence and presence of GABA (Scheller and Forman, 2002). Although α_1M236W and β_2M286W induced qualitatively similar changes, α_1M236W had a significantly greater impact on $GABA_A$ receptor gating.

The remarkably similar impact of these tryptophan mutations compared with etomidate in wild-type receptors supports the hypothesis, based on azi-etomidate photolabeling by Li et al. (2006), that αMet236 and βMet286 project into transmembrane etomidate sites formed at the interfaces between α_1-M1 and β_2-M3 subunits and coupled to channel gating. Although tryptophan was chosen because its side-chain size and hydrophobicity are similar to etomidate, evaluation of additional mutations will help define which side-chain features influence channel gating at these loci.

Contrasting with their similar impact on channel gating, α_1M236W and β_2M286W mutations produced remarkably

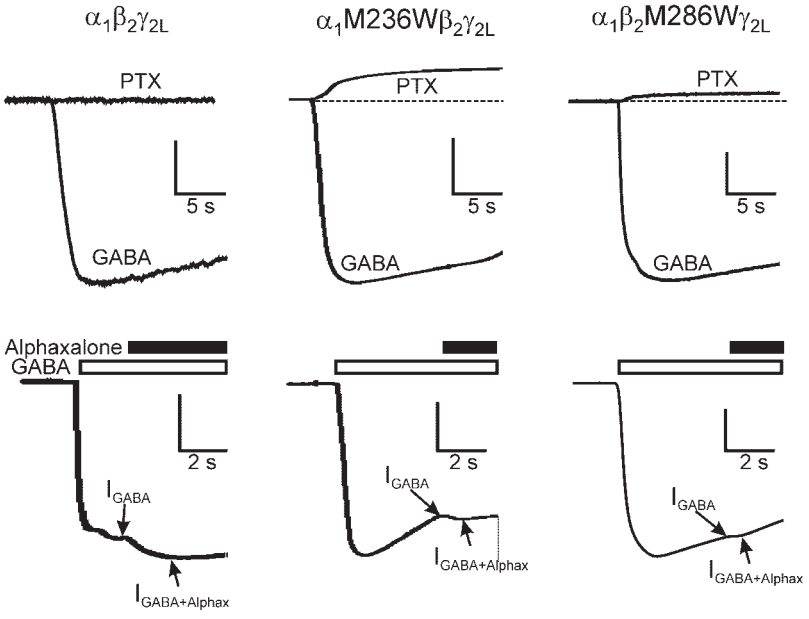

Fig. 3. Estimation of spontaneous activation and maximal GABA efficacy. Sweeps were recorded from oocytes expressing receptors as labeled. Top, examples of current recordings illustrating responses to 2 mM PTX and 10 mM GABA. Wild-type receptors display no detectable PTX-sensitive spontaneous leak current. α_1M236W$\beta_2\gamma_{2L}$ and $\alpha_1\beta_2$M286Wγ_{2L} receptors both display outward currents, representing closure of spontaneously open channels. Results are summarized in Table 1. Bottom, examples of current recordings during multisolution experiments designed to estimate maximal GABA gating efficacy. Currents were initially elicited with 10 mM GABA (I_{GABA}), and 2 μM alphaxalone was then added after the maximal GABA response was observed ($I_{GABA+Alphax}$). Note that alphaxalone enhances wild-type currents by approximately 20%, and much less enhancement (1% or less) is seen in currents elicited from the mutant channels. Estimated GABA efficacies are summarized in Table 1.

different changes in etomidate-dependent effects. Based on GABA EC_{50} shift ratios, β_2M286W eliminated etomidate-induced GABA modulation, while α_1M236W$\beta_2\gamma_{2L}$ receptors displayed a much smaller EC_{50} shift ratio compared with wild-type (2-fold versus 23-fold). Thus, β_2M286W produced a larger impact than α_1M236W on GABA modulation by etomidate. Moreover, etomidate was a highly efficacious direct agonist in α_1M236W$\beta_2\gamma_{2L}$ receptors, displaying the same efficacy as GABA, whereas etomidate has less than half the efficacy of GABA in wild-type receptors and zero agonist efficacy in $\alpha_1\beta_2$M286Wγ_{2L} receptors.

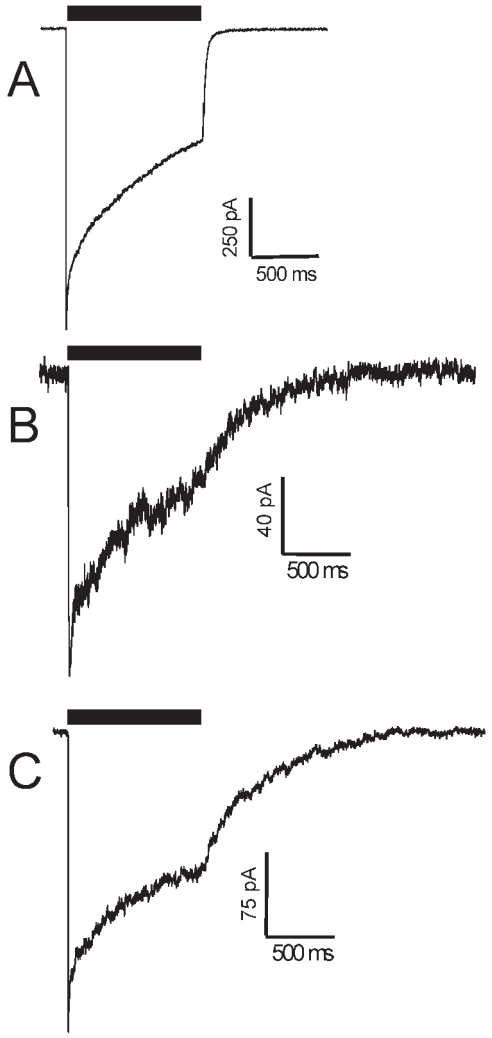

Fig. 4. Activation, desensitization, and deactivation kinetics. Current traces recorded from an HEK293 patch subjected to a 1.0-s GABA pulse (1–3 mM). Black bars over traces represent GABA application period. A, Wild type $\alpha_1\beta_2\gamma_{2L}$ receptors. B, α_1M236W$\beta_2\gamma_{2L}$ receptors. C, $\alpha_1\beta_2$M286Wγ_{2L} receptors. Current activation and desensitization rates are similar for all three traces, whereas deactivation of both mutants is significantly slower than wild type. Average time constants results are reported in Table 2.

That both α_1M236W and β_2M286W weaken etomidate potentiation of GABA activation could be due to steric hindrance reducing etomidate occupation of its site. In the case of β_2M286W, which completely eliminates GABA modulation by etomidate, our data provide no basis for distinguishing whether binding or efficacy of etomidate is eliminated. The β_2Met286 residue and its role in propofol and propofol analog effects on $\alpha_1\beta_2\gamma_{2S}$ $GABA_A$ receptors was studied in detail by Krasowski et al. (2001), who concluded that modulation of GABA currents was dependent on the total volume of the β_2Met286 side-chain and anesthetic drug. When substituted with a cysteine, β_2M286C is accessible to modification by the water-soluble reagent *para*-chloromercuribenzene sulfonate (Williams and Akabas, 1999). Thus, this residue can be reached via an aqueous pathway, although extremely hydrophobic compounds such as propofol and etomidate may access this site more readily via the lipid membrane. Propofol protects βM286C against *para*-chloromercuribenzene sulfonate modification (Bali and Akabas, 2004), further suggesting that propofol binds near this amino acid.

An alternative explanation for reduced etomidate potentiation of GABA currents in α_1M236W$\beta_2\gamma_{2L}$ receptors is based on lower etomidate efficacy rather than weakened binding. Indeed, reduced positive modulation could be generally associated with enhanced GABA gating efficacy, as previously noted for neuroactive steroids (Bianchi and Macdonald, 2003). In essence, because the mutant channels open more readily than wild-type channels in the presence of GABA, less etomidate binding energy is used to achieve opening of all channels, which is reflected in the smaller EC_{50} shift produced by etomidate. Clearly this correlation does not hold for the β_2M286W mutant, which has a smaller impact than α_1M236W on etomidate-independent gating yet is entirely insensitive to etomidate.

Descriptive analyses of etomidate effects on the mutant channels seem to support opposite conclusions regarding whether one versus two classes of etomidate sites exist on $GABA_A$ receptors. The β_2M286W mutant is insensitive to both etomidate-induced agonist potentiation and direct activation by etomidate, consistent with a single type of site

TABLE 2

Activation, desensitization, and deactivation time constants

Time constants are average ± S.D. determined from non-linear least-squares fits of eq. 4 to traces recorded using rapid patch superfusion. Activation and desensitization data is average ± S.D. from at least five experiments on separate membrane patches. Deactivation data is average ± S.D. from at least seven patches.

Receptor	Activation (τ)	Desensitization (Amp./τ)		Deactivation (Amp./τ)	
		Fast	Slow	Fast	Slow
	ms		*%/ms*		
$\alpha_1\beta_2\gamma_{2L}$	0.47 ± 0.16	20 ± 7.4	80 ± 7.4	68 ± 16	32 ± 16
		27 ± 4.1	1100 ± 450	21 ± 9.8	70 ± 16
α_1M236W$\beta_2\gamma_{2L}$	0.46 ± 0.13	21 ± 3.7	79 ± 3.7		100
		35 ± 16	800 ± 340		410 ± 98*
$\alpha_1\beta_2$M286Wγ_{2L}	0.57 ± 0.12	18 ± 6.2	78 ± 6.2	33 ± 26*	67 ± 26*
		34 ± 19	1200 ± 330	96 ± 33*	430 ± 86*

* Differs from wild type at $P < 0.01$

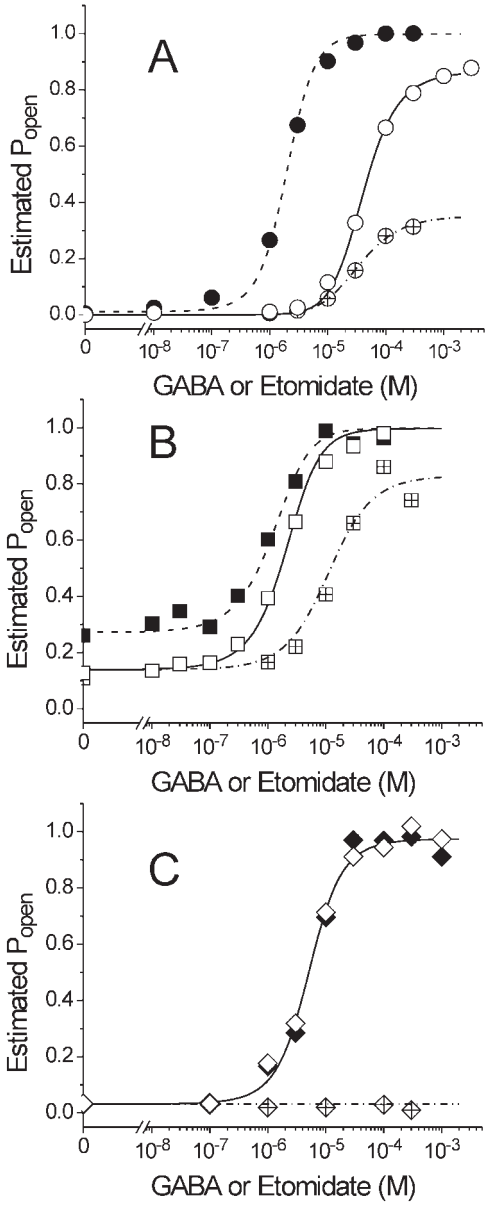

Fig. 5. Monod-Wyman-Changeux coagonist models for GABA and etomidate concentration-responses. Average data from Figs. 1 and 2 (symbols) was transformed into estimated P_o values using eq. 2 in Methods. Equation 3 (Methods) was globally fitted to combined P_o data for each channel with both [GABA] and [ETO] as free parameters. Fitted models are represented by lines through the data points. Solid lines and open symbols represent control GABA responses. Dashed lines and solid symbols represent GABA responses in the presence of 3.2 μM etomidate. Dash-dotted lines and crossed symbols represent etomidate direct activation. A, wild-type $\alpha_1\beta_2\gamma_{2L}$ receptors. B, α_1M236W$\beta_2\gamma_{2L}$ receptors. C, $\alpha_1\beta_2$M286Wγ_{2L} receptors. Fitted parameters are reported in Table 3.

that, when mutated, eliminates both effects. However, the α_1M236W mutation *reduces* etomidate potentiation of GABA activation, while *enhancing* direct activation, suggesting opposite effects at two distinct sites. Nonetheless, the enhanced gating phenotype of α_1M236W$\beta_2\gamma_{2L}$ receptors might also explain the increased sensitivity to etomidate direct activation. As a precedent, we have previously reported that etomidate both potently and efficaciously activates another spontaneously active mutant GABA$_A$ receptor, α_1L264T$\beta_2\gamma_{2L}$ (Rusch et al., 2004). To quantitatively assess whether our results were consistent with a single class of etomidate sites, mechanism-based analysis was performed. We transformed normalized GABA and etomidate concentration-response data (Figs. 1 and 2) into estimated P_o values (eq. 2) and globally fitted the P_o data with eq. 3, which represents an equilibrium Monod-Wyman-Changeux coagonist mechanism. This mechanism incorporates two equivalent etomidate sites per receptor, both allosterically linked to channel opening. Results of the fits are displayed in Fig. 5 and summarized in Table 3.

Quantitative analysis based on the Monod-Wyman-Changeux coagonist mechanism accounted for both wild-type GABA potentiation and direct activation by etomidate (Fig. 5 A), with parameters (Table 3) similar to those previously reported (Rusch et al., 2004). Furthermore, transformed P_o data for the α_1M236W mutant could be fitted with eq. 3, demonstrating that a single class of etomidate sites, with two sites per channel, quantitatively accounts for the effects of this mutation (Fig. 5B). Based on the fitted model parameters, the small GABA EC_{50} shift ratio in α_1M236W$\beta_2\gamma_{2L}$ receptors is attributed to reduced etomidate efficacy relative to wild-type (efficacy is inversely related to d; Table 3), whereas the potent and efficacious direct activation by etomidate is explained by the mutant's high basal opening probability (inversely related to L_0; Table 3), enabling weak etomidate agonism to activate a very large fraction of channels. Compared with wild type, the fitted model parameters for GABA and etomidate binding to inactive channels (K_G and K_E, respectively) are not significantly altered by α_1M236W, whereas GABA efficacy (inversely related to c) is also weakened by the mutation. Weaker apparent efficacy for GABA in α_1M236W$\beta_2\gamma_{2L}$ relative to wild-type can be explained by the reduced energy required to open the mutant channels and could also result from altered transduction of GABA binding energy via the α_1-M1 domain to the channel gating structures. The Monod-Wyman-Changeux mechanism fit to the transformed β_2M286W data suggests that this mutation, like α_1M236W, has little impact on GABA binding but weakens GABA efficacy (Table 3). Given its spontaneous gating activity, the lack of direct activation by etomidate in $\alpha_1\beta_2$M286Wγ_{2L} receptors is remarkable; even a very weak

TABLE 3

Fitted parameters for Monod-Wyman-Changeux co-agonist models

Model parameters were determined by nonlinear least-squares fitting eq. 3 to estimated P_o data sets derived from Figs. 1 and 2. L_0 is a dimensionless basal equilibrium gating variable, representing the inactive/active ratio in the absence of ligands. K_G and K_E are equilibrium dissociation constants for GABA and etomidate binding to inactive states, and c and d are the respective dimensionless efficacy parameters, representing the ratio of binding constants in active versus inactive states.

Receptor	L_0	K_G	c	K_E	d
		μM		μM	
$\alpha_1\beta_2\gamma_{2L}$	20,000 ± 6100	79 ± 17	0.0028 ± 0.00091	21 ± 4.6	0.0096 ± 0.00057
α_1M236W$\beta_2\gamma_{2L}$	6.2 ± 0.66**	51 ± 12	0.021 ± 0.0022**	24 ± 5.1	0.18 ± 0.019**
$\alpha_1\beta_2$M286Wγ_{2L}	31 ± 16**	32 ± 18*	0.029 ± 0.009**		

* Differs from wild type at $P < 0.05$.
** Differs from wild type at $P < 0.01$.

etomidate efficacy factor of 0.7 to 0.8 should cause a readily observable 20 to 30% increase in the resting leak current of this channel. This suggests that β_2M286W profoundly alters the interaction between receptor and drug, probably by preventing drug binding.

There is accumulating evidence that the α-M1 domain and nearby structures, including pre-M1 residues on α and the adjacent β-M3, contribute to sites for a variety of $GABA_A$ receptor modulators. Evidence for propofol interactions with βMet286 is discussed above. Both channel gating and barbiturate sensitivity are influenced by mutations in α pre-M1 and the proline at the onset of α-M1 (Greenfield et al., 2002; Chang et al., 2003; Mercado and Czajkowski, 2006). Mutations in both α-M1 and β-M3 domains also alter sensitivity to neuroactive steroids (Hosie et al., 2006; Akk et al., 2008). Despite the proximity of multiple residues that influence anesthetic sensitivities, most evidence supports distinct $GABA_A$ receptor sites for different anesthetics. β_2M286W eliminates direct receptor activation by etomidate but not by propofol, barbiturates, and alphaxalone (Krasowski et al., 2001; Siegwart et al., 2002). Receptors containing α_1M236W maintain modulation by both alphaxalone and pentobarbital (our data, not shown). Li et al. (2006) also reported that a neuro-active steroid enhances azi-etomidate photolabeling of $GABA_A$ receptors, indicating a distinct site. A recent report suggests that different neuroactive steroids may interact with different parts of the α-M1 domain yet lead to convergent effects on channel activity (Akk et al., 2008). We speculate that α-M1, β-M3, and other nearby structures form an extensive pocket that changes conformation during gating, perhaps enlarging. In its expanded configuration, this pocket might accommodate a variety of potent anesthetics at different subsites. Similar intrasubunit transmembrane pockets have been postulated for volatile anesthetics and alcohols (Jenkins et al., 2001) and for neuroactive steroids (Hosie et al., 2006).

In conclusion, our results provide critical links between the azi-etomidate photolabeling sites and the molecular actions of etomidate in $GABA_A$ receptors. Etomidate is currently the only general anesthetic for which there are known critical target receptors (Jurd et al., 2003; Reynolds et al., 2003), a working structural model for the molecular sites on these receptors (Li et al., 2006), and a quantitative model for molecular effects mediated by these sites (Rusch et al., 2004). More studies are needed to further delineate the etomidate-binding pocket and to determine whether gating and anesthetic modulation are influenced by the entire α-M1 domain or only residues facing β-M3. Similar tests of other potent anesthetics may also better define their sites of action.

Acknowledgments

We thank Drs. Jonathan Cohen (Harvard Medical School, Boston, MA), David Chiara (Harvard Medical School, Boston, MA), and Keith Miller (Massachusetts General Hospital, Boston, MA) for their comments and suggestions.

References

Akk G, Li P, Bracamontes J, Reichert DE, Covey DF, and Steinbach JH (2008) Mutations of the GABA-A receptor α1 subunit M1 domain reveal unexpected complexity for modulation by neuroactive steroids. *Mol Pharmacol* **74:**614–627.

Bali M and Akabas MH (2004) Defining the propofol binding site location on the GABAA receptor. *Mol Pharmacol* **65:**68–76.

Baumann SW, Baur R, and Sigel E (2002) Forced subunit assembly in $\alpha_1\beta_2\gamma_2$ $GABA_A$ receptors. Insight into the absolute arrangement. *J Biol Chem* **277:**46020–46025.

Bianchi MT and Macdonald RL (2003) Neurosteroids shift partial agonist activation of GABAA receptor channels from low- to high-efficacy gating patterns. *J Neurosci* **23:**10934–10943.

Boileau AJ, Baur R, Sharkey LM, Sigel E, and Czajkowski C (2002) The relative amount of cRNA coding for gamma2 subunits affects stimulation by benzodiazepines in GABA(A) receptors expressed in *Xenopus* oocytes. *Neuropharmacology* **43:**695–700.

Boileau AJ, Li T, Benkwitz C, Czajkowski C, and Pearce RA (2003) Effect of γ2S subunit incorporation on GABAA receptor macroscopic kinetics. *Neuropharmacology* **44:**1003–1012.

Chang CS, Olcese R, and Olsen RW (2003) A single M1 residue in the β2 subunit alters channel gating of $GABA_A$ receptor in anesthetic modulation and direct activation. *J Biol Chem* **278:**42821–42828.

Chang Y, Wang R, Barot S, and Weiss DS (1996) Stoichiometry of a recombinant GABAA receptor. *J Neurosci* **16:**5415–5424.

Chang Y and Weiss DS (1999) Allosteric activation mechanism of the alpha1beta2gamma2 gamma-aminobutyric acid type A receptor revealed by mutation of the conserved M2 leucine. *Biophys J* **77:**2542–2551.

Findlay GS, Ueno S, Harrison NL, and Harris RA (2001) Allosteric modulation in spontaneously active mutant gamma-aminobutyric acidA receptors. *Neurosci Lett* **305:**77–80.

Greenfield LJ Jr, Zaman SH, Sutherland ML, Lummis SC, Niemeyer MI, Barnard EA, and Macdonald RL (2002) Mutation of the GABAA receptor M1 transmembrane proline increases GABA affinity and reduces barbiturate enhancement. *Neuropharmacology* **42:**502–521.

Hill-Venning C, Belelli D, Peters JA, and Lambert JJ (1997) Subunit-dependent interaction of the general anaesthetic etomidate with the gamma-aminobutyric acid type A receptor. *Br J Pharmacol* **120:**749–756.

Hosie AM, Wilkins ME, da Silva HM, and Smart TG (2006) Endogenous neurosteroids regulate GABAA receptors through two discrete transmembrane sites. *Nature* **444:**486–489.

Husain SS, Ziebell MR, Ruesch D, Hong F, Arevalo E, Kosterlitz JA, Olsen RW, Forman SA, Cohen JB, and Miller KW (2003) 2-(3-Methyl-3H-diaziren-3-yl)ethyl 1-(1-phenylethyl)-1H-imidazole-5-carboxylate: a derivative of the stereoselective general anesthetic etomidate for photolabeling ligand-gated ion channels. *J Med Chem* **46:**1257–1265.

Jenkins A, Greenblatt EP, Faulkner HJ, Bertaccini E, Light A, Lin A, Andreasen A, Viner A, Trudell JR, and Harrison NL (2001) Evidence for a common binding cavity for three general anesthetics within the GABAA receptor. *J Neurosci* **21:** RC136.

Jurd R, Arras M, Lambert S, Drexler B, Siegwart R, Crestani F, Zaugg M, Vogt KE, Ledermann B, Antkowiak B, et al. (2003) General anesthetic actions in vivo strongly attenuated by a point mutation in the GABA(A) receptor beta3 subunit. *FASEB J* **17:**250–252.

Krasowski MD, Hong X, Hopfinger AJ, and Harrison NL (2002) 4D-QSAR analysis of a set of propofol analogues: mapping binding sites for an anesthetic phenol on the GABA(A) receptor. *J Med Chem* **45:**3210–3221.

Krasowski MD, Koltchine VV, Rick CE, Ye Q, Finn SE, and Harrison NL (1998) Propofol and other intravenous anesthetics have sites of action on the γ-aminobutyric acid type A receptor distinct from that for isoflurane. *Mol Pharmacol* **53:**530–538.

Krasowski MD, Nishikawa K, Nikolaeva N, Lin A, and Harrison NL (2001) Methionine 286 in transmembrane domain 3 of the GABAA receptor beta subunit controls a binding cavity for propofol and other alkylphenol general anesthetics. *Neuropharmacology* **41:**952–964.

Li GD, Chiara DC, Sawyer GW, Husain SS, Olsen RW, and Cohen JB (2006) Identification of a GABAA receptor anesthetic binding site at subunit interfaces by photolabeling with an etomidate analog. *J Neurosci* **26:**11599–11605.

Liao M, Sonner JM, Husain SS, Miller KW, Jurd R, Rudolph U, and Eger EI 2nd (2005) R (+) etomidate and the photoactivable R (+) azietomidate have comparable anesthetic activity in wild-type mice and comparably decreased activity in mice with a N265M point mutation in the gamma-aminobutyric acid receptor beta3 subunit. *Anesth Analg* **101:**131–135.

Majewska MD, Harrison NL, Schwartz RD, Barker JL, and Paul SM (1986) Steroid hormone metabolites are barbiturate-like modulators of the GABA receptor. *Science* **232:**1004–1007.

Mercado J and Czajkowski C (2006) Charged residues in the alpha1 and beta2 pre-M1 regions involved in GABAA receptor activation. *J Neurosci* **26:**2031–2040.

Reynolds DS, Rosahl TW, Cirone J, O'Meara GF, Haythornthwaite A, Newman RJ, Myers J, Sur C, Howell O, Rutter AR, et al. (2003) Sedation and anesthesia mediated by distinct GABA(A) receptor isoforms. *J Neurosci* **23:**8608–8617.

Rüsch D and Forman SA (2005) Classic benzodiazepines modulate the open-close equilibrium in alpha1beta2gamma2L gamma-aminobutyric acid type A receptors. *Anesthesiology* **102:**783–792.

Rüsch D, Zhong H, and Forman SA (2004) Gating allosterism at a single class of etomidate sites on $\alpha_1\beta_2\gamma_{2L}$ $GABA_A$ receptors accounts for both direct activation and agonist modulation. *J Biol Chem* **279:**20982–20992.

Scheller M and Forman SA (2002) Coupled and uncoupled gating and desensitization effects by pore domain mutations in GABA(A) receptors. *J Neurosci* **22:**8411–8421.

Serafini R, Bracamontes J, and Steinbach JH (2000) Structural domains of the human GABAA receptor beta3 subunit involved in the actions of pentobarbital. *J Physiol* **524:**649–676.

Sieghart W (2006) Structure, pharmacology, and function of GABAA receptor subtypes. *Adv Pharmacol* **54:**231–263.

Siegwart R, Jurd R, and Rudolph U (2002) Molecular determinants for the action of general anesthetics at recombinant alpha(2)beta(3)gamma(2)gamma-aminobutyric acid(A) receptors. *J Neurochem* **80:**140–148.

Williams DB and Akabas MH (1999) Gamma-aminobutyric acid increases the water accessibility of M3 Membrane-spanning segment residues in GABA-A receptors. *Biophys J* **77:**2563–2574.

Yang J and Uchida I (1996) Mechanisms of etomidate potentiation of GABAA receptor-gated currents in cultured postnatal hippocampal neurons. *Neuroscience* **73:**69–78.

Zhong H, Rüsch D, and Forman SA (2008) Photo-activated azi-etomidate, a general anesthetic photolabel, irreversibly enhances gating and desensitization of gamma-aminobutyric acid type A receptors. *Anesthesiology* **108:**103–112.

Address correspondence to: Dr. Stuart A. Forman, Beecher/Mallincrodt Labs, Dept. of Anesthesia and Critical Care, Gray-Jackson 4, Mass. General Hospital, 55 Fruit Street, Boston, MA 02114. E-mail: saforman@partners.org